Comprehensive Radiation Testing of Uncooled, Free Space Coupled, InGaAs Quad Photoreceivers

Abhay M. Joshi*[1], Shubhashish Datta[1], Nilesh Soni[1], Matthew D'Angiolillo[1], Jeff Mertz[1], Michael Sivertz[2], Adam Rusek[2], James Jardine[3], and Jeff Livas[4]

[1] Discovery Semiconductors Inc., Ewing, NJ, USA;
[2] NASA Space Radiation Laboratory, Brookhaven National Laboratory, Upton, NY, USA;
[3] Brookhaven National Laboratory, Upton, NY, USA;
[4] NASA Goddard Space Flight Center, Greenbelt, MD, USA.

ABSTRACT

We have comprehensively tested uncooled, free space coupled, InGaAs Quad Photoreceivers having 0.5 mm, 1 mm, and 2 mm diameter integrated with a low noise transimpedance amplifier (TIA) using 30 MeV Protons, 100 MeV Protons, 662 keV Gamma Rays, 1 GeV/n Helium, and 1 GeV/n Iron at room temperature of ~20 °C. These devices find multiple applications in space for differential wavefront sensing as part of a Gravitational Wave Observatory, as well as instrumentation and control for next generation space telescopes. The bandwidth of all receivers was 20 MHz which was TIA limited.

All 0.5 mm and 1 mm devices were found to be fully functional at normal operating conditions and at room temperature for Protons, Gamma Rays, 1 GeV/n Helium, and 1 GeV/n Iron. Only one quadrant of a 2 mm InGaAs Quad had hard failure due to 1 GeV/n Helium Ions; otherwise it too survived all other radiation tests. Detailed test results follow in the manuscript including recommendations for future space flights. These radiation test results, combined with the earlier successful mechanical shock and vibration testing mean these devices have passed preliminary testing for space qualification.

Keywords: InGaAs photodiodes, quadrant photodetector, proton, gamma rays, 1 GeV/n He, 1 GeV/n Fe, radiation, gravitational wave sensing.

1. INTRODUCTION

Photodetectors have been deployed in satellites for low-speed passive sensing applications for decades. Photonics is expected to increase its role significantly in space platforms, which requires higher optical power handling for coherent systems and/or higher speed, than previously satisfied by mature space technologies, such as cooled Mercury Cadmium Telluride (MCT) photodetectors. High performance Indium Gallium Arsenide (InGaAs) photodetectors, which are appropriate for such applications, are yet to be utilized to their full potential in space systems due to a dearth of radiation test data needed for space qualification. InGaAs photodetectors can also be operated uncooled at ~20 °C in coherent systems, which significantly improves the SWaP considerations in the spacecraft design.

One such device is the uncooled, free space coupled, InGaAs Quad Photoreceiver that we previously developed for space-based gravitational wave detection through coherent optical wavefront sensing [1, 2]. These devices have been shown to satisfy stringent signal-to-noise requirements of the Laser Interferometry Space Antenna (LISA) mission, and have recently passed MIL-STD-883 mechanical shock and sinusoidal vibration tests [3].

In this work, we present the radiation test results of InGaAs Quad Photoreceivers having 0.5 mm, 1 mm, and 2 mm diameter for 30 MeV Protons, 100 MeV Protons, 662 keV Gamma Rays, 1 GeV/n Helium, and 1 GeV/n Iron. These tests were performed at ~20 °C, in line with the operating temperature of the LISA mission. We also analyze the dependence of susceptibility to radiation on device size, which provides valuable insight for the system designers. Combined with our concurrent radiation testing of other types of uncooled InGaAs photodetectors [4, 5], this work will expand induction of photonics in space.

* amjoshi@discoverysemi.com; phone +1 609 434 1311; fax +1 609 434 1317; www.discoverysemi.com

2. ULTRA-LOW NOISE InGaAs QUAD PHOTORECEIVER

A Quad Photoreceiver is a 2 x 2 array of p-i-n photodiodes followed by a transimpedance amplifier (TIA) per diode, as shown in Fig. 1a. It is desirable to increase the active area of free space coupled, Quad Photodiodes to collect more optical signal and enhance the RF signal levels. However, increasing a photodiode's active area leads to a commensurate increase in its capacitance. Coupled with the TIA's input voltage noise, this capacitance generates a noise term that linearly scales with the optical collection efficiency [6]. Consequently, increasing the photodiode's active area may not improve the signal-to-noise ratio in the system, in spite of enhanced link gain. Therefore, it is necessary to minimize the capacitance of large-area Quad Photodiodes to realize low-noise, large-area Quad Photoreceivers. It is also desirable to minimize the dead zone between the photodiode quadrants to increase the optical collection area and improve the signal to noise ratio in wavefront sensing systems.

We have previously developed a 1 mm diameter, InGaAs Quad Photodiode having 2.5 pF capacitance per quadrant, which was used to manufacture an ultra-low noise Quad Photoreceiver for the LISA mission. Such a low capacitance constitutes an 8-fold improvement over comparable devices. The neighboring photodiode quadrants are separated by 20 µm, thus reducing the dead zone by a factor 4 to 5 as compared to typical devices. Each quadrant of the Quad Photodiode was coupled to a low noise, Silicon Bipolar OpAmp-based TIA circuit to realize the Quad Photoreceiver. The Quad Photoreceiver was assembled in a standard TO-3 package with a Sapphire window, which was anti-reflection coated for 1064 nm wavelength. The TIA circuit was designed to meet the specifications of the LISA mission, and was optimized for 2 to 20 MHz operation. As shown in Figs. 1b & 1c, a 1 mm diameter Quad Photoreceiver achieves an equivalent input current noise density of <1.7 pA/√Hz per quadrant up to a -3 dB bandwidth of ~20 MHz at ~20 °C operating temperature [1].

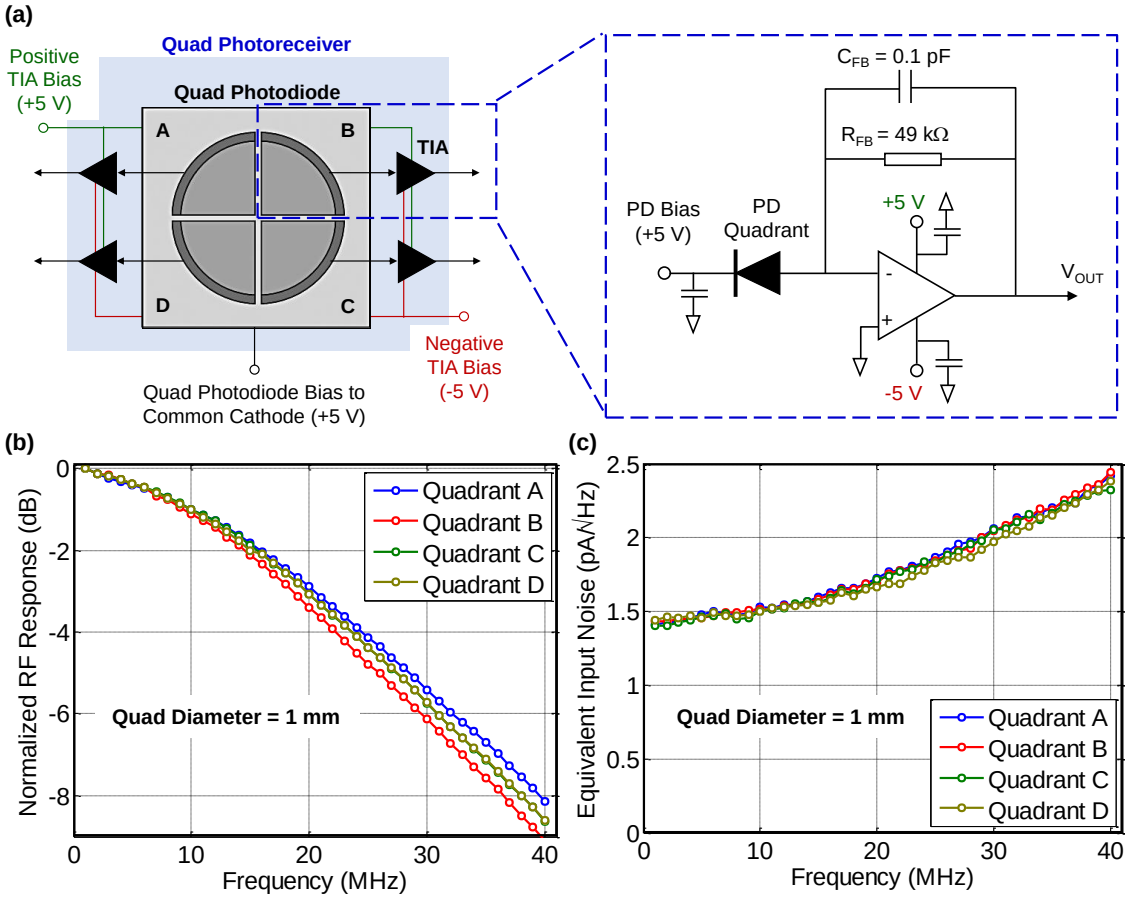

Figure 1. **(a)** Schematic of a InGaAs Quad PD + TIA Photoreceiver. **(b)** Normalized RF response and **(c)** equivalent input current noise density of each quadrant of the 1 mm diameter Quad Photoreceiver at ~20 °C temperature [1].

For this work, we assembled 0.5 mm, 1 mm, and 2 mm diameter Quad Photoreceivers with the objective of quantifying the effect of photodiode size on resilience to radiation. All the Quad Photodiode dies were co-processed on the same epitaxially-grown InGaAs wafer that consistently demonstrates a capacitance per unit area of 12.7 pF/mm^2 at 5 V reverse bias, as shown in Fig. 2. The worst-case noise density, defined at the highest frequency of interest, proportionally scales with the capacitance and the area of the photodiode quadrant [6]. Therefore, 2 mm diameter Quad Photoreceivers demonstrate 4x higher noise than 1 mm devices.

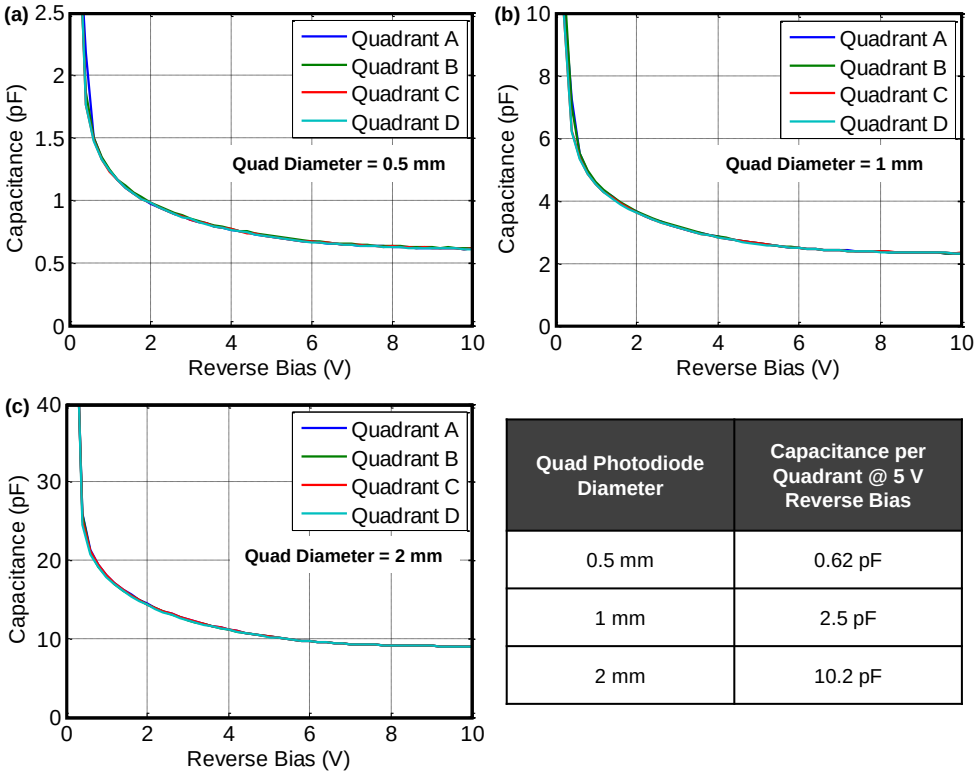

Quad Photodiode Diameter	Capacitance per Quadrant @ 5 V Reverse Bias
0.5 mm	0.62 pF
1 mm	2.5 pF
2 mm	10.2 pF

Figure 2. Capacitance per quadrant as a function of reverse bias for InGaAs Quad Photodiodes having a diameter of **(a)** 0.5 mm, **(b)** 1 mm, and **(c)** 2 mm. Capacitance per quadrant at the operating reverse bias of 5 V is annotated.

3. OVERVIEW OF RADIATION TESTS

One Quad Photoreceiver of each diameter was subjected to the following radiation tests:

- 30 MeV Protons with fluence levels of 4.92×10^{10} cm^{-2}, 9.84×10^{10} cm^{-2}, and 1.64×10^{11} cm^{-2};
- 100 MeV Protons with fluence levels of 1.27×10^{11} cm^{-2}, 2.54×10^{11} cm^{-2}, and 4.23×10^{11} cm^{-2};
- 1 GeV/n Fe Ion with fluence level of 2.8×10^{5} cm^{-2};
- 1 GeV/n He Ion with fluence level of 1.4×10^{8} cm^{-2}; and
- 662 keV Gamma rays with Total Ionizing Dose (TID) of 15 krad (water) and 30 krad (water).

All radiation test setups were designed to irradiate three unbiased Quad Photoreceivers simultaneously with consistent flux levels at ambient room temperature. It has been shown that the displacement damage is the key failure mechanism in InGaAs/InP photodiodes, and is independent of the in-situ biasing of the devices during radiation [7, 8].

The Quad Photodiode dark current, combined drive current of the four TIA circuits, and the output noise density per quadrant were measured for each device at nominal room temperature, before and after every radiation test. It should be noted that output noise density unchanged by radiation shows the resilience of the TIA's input equivalent noise as well as the transfer function of the Quad Photoreceivers. Any device that demonstrated >2-fold increase in Quad Photodiode dark current was considered to have soft failure and was withdrawn from further tests, even if it was functional and displayed consistent output noise density with no significant degradation in SNR. As shown in Fig. 3, five sets of devices were used for the ten radiation tests that are described in the remainder of this manuscript.

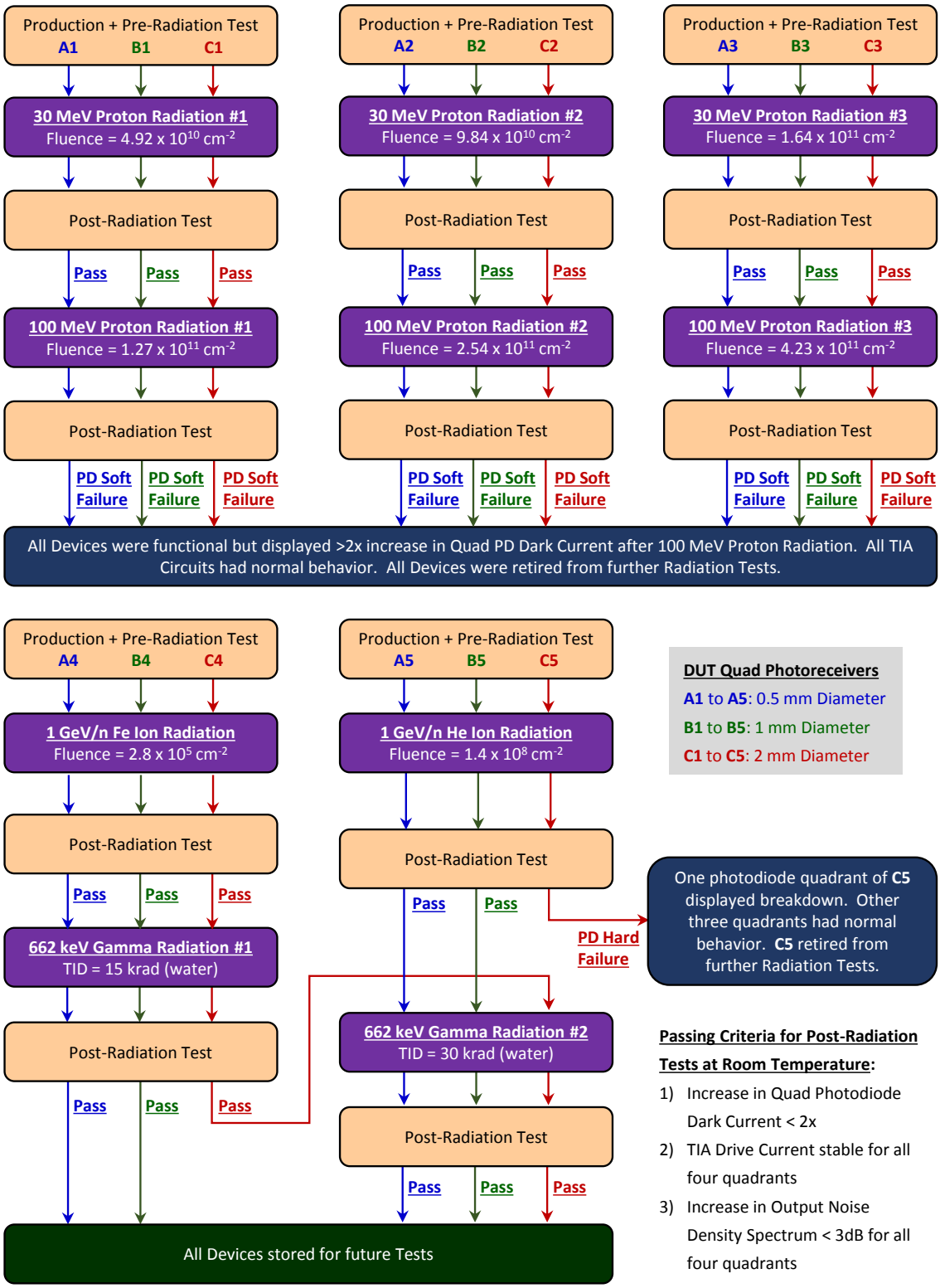

Figure 3. Overview of 30 MeV Proton, 100 MeV Proton, 1 GeV/n Fe Ion, 1 GeV/n He Ion, and 662 keV Gamma Radiation Tests performed on uncooled, free space coupled, InGaAs Quad Photoreceivers having 0.5 mm, 1 mm, and 2 mm diameter.

4. 30 MeV and 100 MeV PROTON RADIATION TESTS

Our measurement campaign started with 30 MeV proton radiation experiments. Three InGaAs Quad Photoreceivers of each diameter were manufactured for these tests. These devices were irradiated with protons in the setup shown in Fig. 4a at the NASA Space Radiation Laboratory at Brookhaven National Laboratory (BNL) in Upton, New York. The protons were provided by the BNL Tandem Van de Graaff, and transported to the Booster synchrotron where they were accelerated to 100 MeV. A 68.3 mm thick polyethylene degrader was used to slow the protons down to 30 MeV with an energy spread of ~4 MeV. The entire beam was extracted from the Booster in about 400 milliseconds for a "spill" every 4 to 6 seconds. Once extracted, the protons were directed through an external beam line to produce a large square beam spot. The central region of the beam spot was tuned to be approximately 5×5 cm^2, which allowed simultaneously irradiating up to 3 devices at normal incidence angle, as shown in Fig. 4b. The radiation field variation was less than 3% across the target area. The beam was imaged with a fluorescent screen and viewed by a CCD camera, giving instantaneous life-sized images of the beam profile, spill by spill. The total fluence was measured using a large planar ion chamber between the vacuum window of the beamline and the photoreceivers. The ion chamber was calibrated by measuring the response of the ion chamber at the same time as a calibration chamber, which was placed at the location to be used by the photoreceivers. The calibration chamber is a 1 cm^3 spherical ion chamber that is periodically sent to a NIST-traceable laboratory, where its calibration is checked by exposing it to a Cesium-137 gamma source.

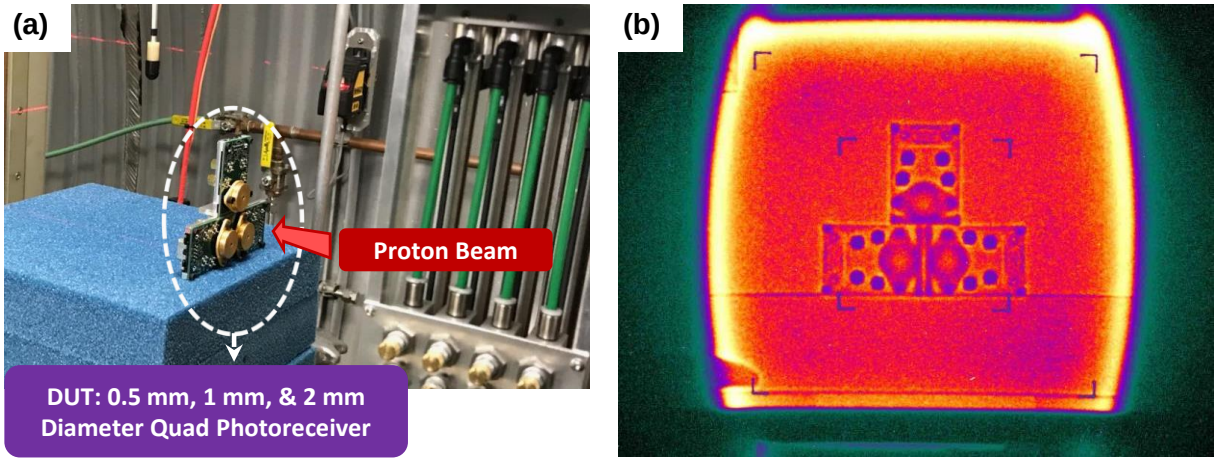

Figure 4. **(a)** Photograph of 0.5 mm, 1 mm, and 2 mm diameter InGaAs Quad Photoreceivers in the experimental setup for Proton radiation at the NASA Space Radiation Laboratory. The devices were unbiased and were kept at ambient room temperature during the exposures to normally incident Proton beam. **(b)** Proton radiation beam profile showing the footprint of three devices being simultaneously radiated with uniform flux.

The key parameters of the three 30 MeV proton radiation tests are summarized in Table I. The highest dose of 1.6×10^{11} cm^{-2} corresponds to a typical 10+ year-long space mission [9]. After exposure to proton radiation, the photoreceivers were found to be slightly activated, and placed in a holding cell to decay to the background radiation level prior to post-radiation testing. The test results of these devices before and after 30 MeV proton radiation are summarized in Tables II and III, respectively. Their output noise spectra are shown in Figs. 5 and 6.

Table I. 30 MeV Proton Radiation Test Parameters

Proton Energy	Average Flux	Irradiation Time	Fluence Level	DUT Quad Photoreceiver ID		
				0.5 mm	1 mm	2 mm
30 MeV	3.1×10^7 cm^{-2}s^{-1}	1571 s	4.92×10^{10} cm^{-2}	A1	B1	C1
		3103 s	9.84×10^{10} cm^{-2}	A2	B2	C2
		6549 s	1.64×10^{11} cm^{-2}	A3	B3	C3

Table II. Quad Photoreceiver Results before Proton Radiation

Device: Quad Diameter	Total PD Dark Current @ 5V Bias (nA)	Total Amplifier Current @ ±5V Bias (mA)	Output Noise Density (nV/√Hz) per Quadrant @ 20 MHz			
			A	B	C	D
A1: 0.5 mm	36	26.2	42.3	40.8	40.7	41.9
A2: 0.5 mm	35	26.9	41.6	40.4	40.4	39.8
A3: 0.5 mm	32	26.5	42.3	41.3	39.8	40.9
B1: 1 mm	112	26.6	64.6	63.5	62.4	61.7
B2: 1 mm	122	26.7	65.6	67.1	64.5	63.9
B3: 1 mm	110	26.4	64.3	64.3	64.5	63.2
C1: 2 mm	225	26.5	315.1	285.9	299.0	300.5
C2: 2 mm	302	26.2	296.1	331.1	328.2	280.0
C3: 2 mm	280	26.3	258.2	293.2	278.6	258.2

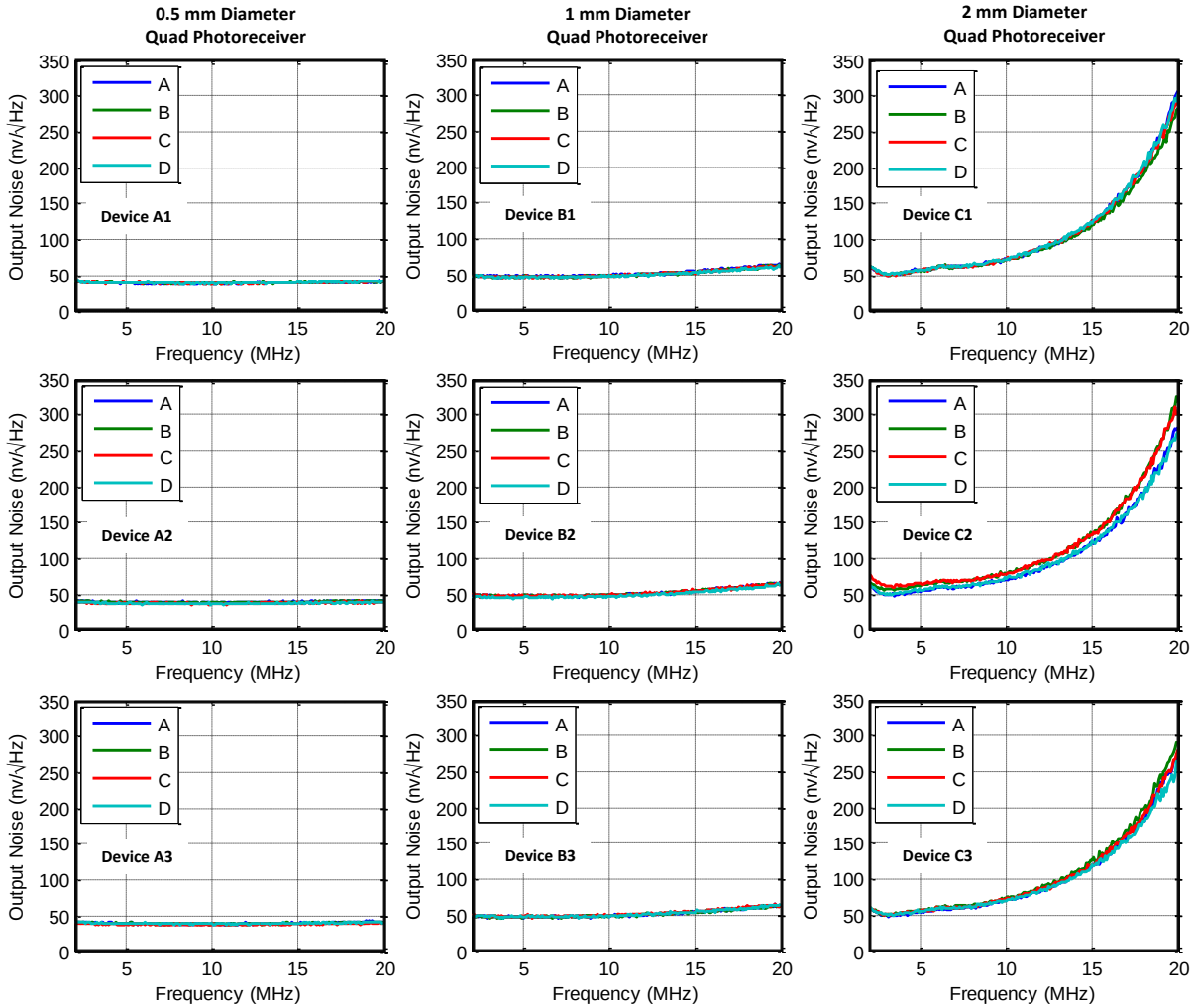

Figure 5. Output noise density spectra of Quad Photoreceivers before proton radiation. **Note:** Minor fluctuations in dark current and output noise are observed as average room temperature is 19.5 °C ± 2 °C.

Table III. Quad Photoreceiver Results after 30 MeV Proton Radiation

Device: Quad Diameter	30 MeV Proton Fluence	Total PD Dark Current @ 5V Bias (nA)	Total Amplifier Current @ ±5V Bias (mA)	Output Noise Density (nV/√Hz) per Quadrant @ 20 MHz			
				A	B	C	D
A1: 0.5 mm	4.92×10^{10} cm^{-2}	37	26.5	41.7	42.1	42.2	42.2
A2: 0.5 mm	9.84×10^{10} cm^{-2}	41	26.7	42.3	42.4	40.3	39.4
A3: 0.5 mm	1.64×10^{11} cm^{-2}	49	26.5	42.4	41.4	40.7	41.9
B1: 1 mm	4.92×10^{10} cm^{-2}	120	26.6	69.9	63.6	63.6	63.9
B2: 1 mm	9.84×10^{10} cm^{-2}	130	26.6	67.4	67.2	66.7	64.9
B3: 1 mm	1.64×10^{11} cm^{-2}	134	26.4	65.5	65.2	66.1	65.3
C1: 2 mm	4.92×10^{10} cm^{-2}	229	26.5	317.9	294.6	301.9	304.8
C2: 2 mm	9.84×10^{10} cm^{-2}	320	26.7	293.2	336.9	325.3	288.8
C3: 2 mm	1.64×10^{11} cm^{-2}	380	26.5	294.6	306.3	297.6	275.7

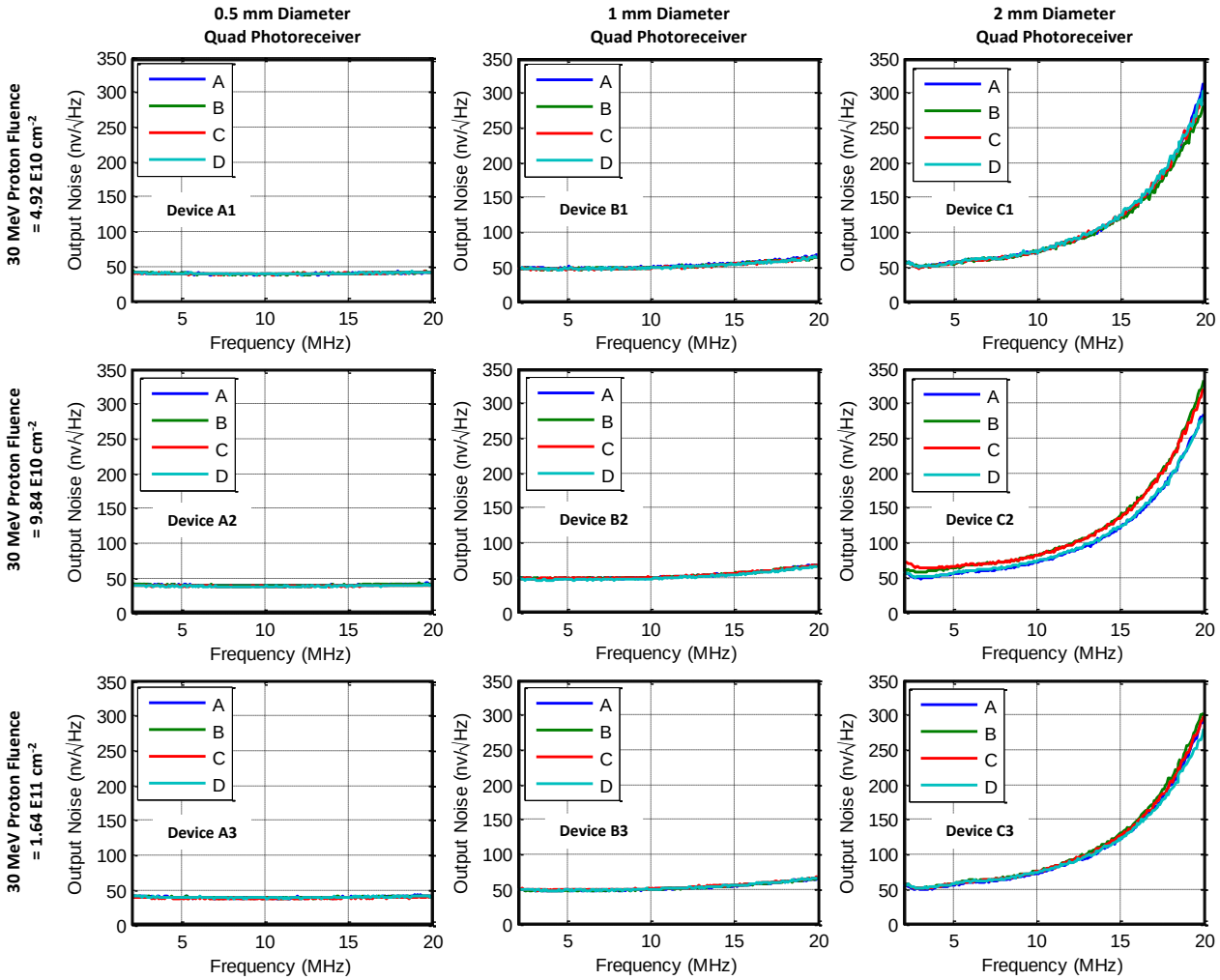

Figure 6. Output noise density spectra of Quad Photoreceivers after 30 MeV proton radiation. **Note:** Minor fluctuations in dark current and output noise are observed as average room temperature is 19.5 °C ± 2 °C.

Comparing the device performance before and after 30 MeV proton radiation, the following observations can be made:

1. The Quad Photodiode's dark current is virtually the same for the lowest fluence level considering ±2 °C variation in the room temperature. As expected, the increase in dark current was most pronounced for the highest fluence of 1.64×10^{11} cm^{-2}. This increase is due to displacement damage in the InGaAs photodiode that contributes to both bulk and surface components of the dark current. However, the post-radiation dark currents were stable and within 2x margin with respect to the pre-radiation data for every device.
2. The drive currents of the TIAs were unchanged for every device.
3. Finally, the output noise density results were essentially unchanged for all devices.

Having passed the 30 MeV Proton radiation tests, these nine devices were further subjected to 100 MeV protons in the same radiation setup shown in Fig. 4. The polyethylene degrader was omitted to create 100 MeV proton beam with an energy spread of ±0.5 MeV. The geometry of the radiation setup, including beam spot size, beam uniformity, and orientation of the DUT Quad Photoreceivers with respect to the beam, was kept consistent with the 30 MeV proton experiments. The key parameters of the three 100 MeV proton radiation tests are summarized in Table IV.

Table IV. 100 MeV Proton Radiation Test Parameters

Proton Energy	Average Flux	Irradiation Time	Fluence Level	DUT Quad Photoreceiver ID		
				0.5 mm	1 mm	2 mm
100 MeV	5.5×10^7 $cm^{-2}s^{-1}$	2903 s	1.27×10^{11} cm^{-2}	A1	B1	C1
		4618 s	2.54×10^{11} cm^{-2}	A2	B2	C2
		7691 s	4.23×10^{11} cm^{-2}	A3	B3	C3

The fluence levels used in our experiments are significantly higher than that expected for a typical space mission. For example, the LISA mission anticipates a 100 MeV Proton fluence of 5.71×10^7 cm^{-2} for an extended 7-year mission [9]. Thus, the highest fluence level corresponds to 260-year mission with a 2x design margin. Remarkably, all devices were functional after undergoing the 100 MeV Proton tests.

The photodiode dark current increased significantly for all devices as compared to the numbers reported in Table III due to radiation-induced displacement damage. This is in line with our prior observation of increased tunneling current in 10 GHz bandwidth, InGaAs photoreceivers that were subjected to 100 MeV protons [4]. As summarized in Table V, the displacement damage in the InGaAs photodiode increases monotonically with device size for all 100 MeV proton fluence levels, thus demonstrating increased susceptibility of larger devices to radiation.

Although no significant change was observed in the TIA drive current and the output noise density, as shown in Table VI and Fig. 7, all these devices were retired from further radiation testing as their dark current demonstrated >2-fold increase.

Table V. Percentage Increase in Quad Photodiode Dark Current at Room Temperature due to 100 MeV Proton Radiation

100 MeV Proton Fluence Level	Quad Diameter		
	0.5 mm	1 mm	2 mm
1.27×10^{11} cm^{-2}	160%	190%	310%
2.54×10^{11} cm^{-2}	260%	320%	1580%
4.23×10^{11} cm^{-2}	350%	460%	830%

Table VI. Quad Photoreceiver Results after 100 MeV Proton Radiation

Device: Quad Diameter	100 MeV Proton Fluence	Total PD Dark Current @ 5V Bias (nA)	Total Amplifier Current @ ±5V Bias (mA)	Output Noise Density (nV/√Hz) per Quadrant @ 20 MHz			
				A	B	C	D
A1: 0.5 mm	1.27×10^{11} cm^{-2}	96	26.7	42.4	43.0	43.3	42.7
A2: 0.5 mm	2.54×10^{11} cm^{-2}	174	27.0	43.0	42.7	41.1	41.4
A3: 0.5 mm	4.23×10^{11} cm^{-2}	220	26.7	42.7	42.7	42.7	42.1
B1: 1 mm	1.27×10^{11} cm^{-2}	342	26.8	68.3	67.0	65.8	66.1
B2: 1 mm	2.54×10^{11} cm^{-2}	543	26.9	67.0	67.4	65.8	67.7
B3: 1 mm	4.23×10^{11} cm^{-2}	750	27.3	66.7	67.0	67.4	67.4
C1: 2 mm	1.27×10^{11} cm^{-2}	935	26.7	322.6	295.0	304.2	301.0
C2: 2 mm	2.54×10^{11} cm^{-2}	5390	26.9	287.8	325.7	325.7	291.9
C3: 2 mm	4.23×10^{11} cm^{-2}	3540	26.7	312.1	322.5	290.3	306.1

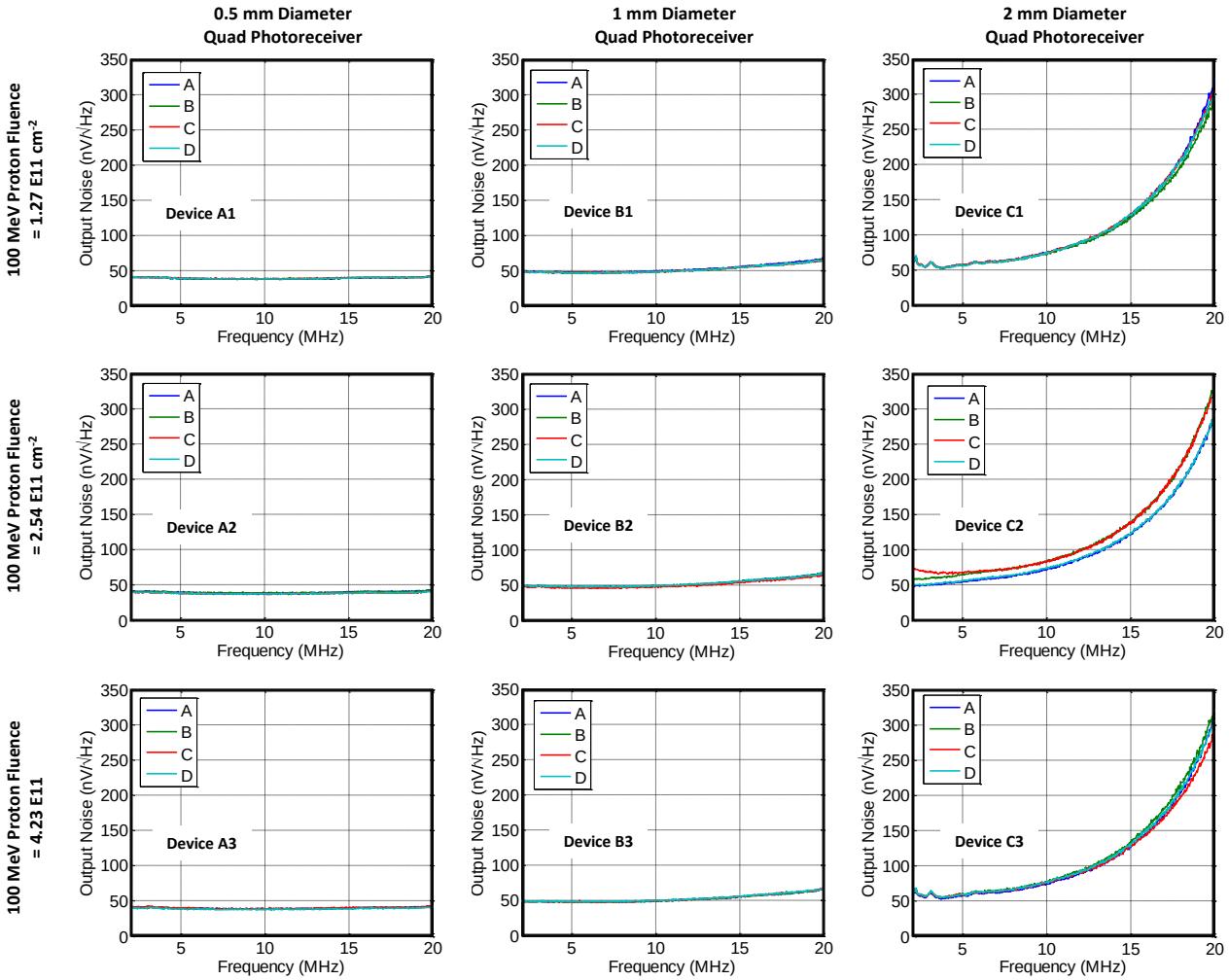

Figure 7. Output noise density spectra of Quad Photoreceivers after 100 MeV proton radiation. **Note:** Minor fluctuations in dark current and output noise are observed as average room temperature is 19.5 °C ± 2 °C.

5. GALACTIC COSMIC RAY CONSITUENT ION RADIATION TESTS

Galactic cosmic ray (GCR) nuclei are a significant component of the space radiation environment for outer space missions beyond the Earth's magnetosphere. The nuclear composition of GCR includes all the elements of the periodic table from Hydrogen to Uranium. Although the majority of the cosmic rays is comprised of Hydrogen and Helium, heavier elements such as Iron make a greater contribution to the dose equivalent due to higher rate of energy loss [10]. Also, ~75% of the dose equivalent is due to the cosmic ray nuclei with energy < 1 GeV/n. Based on the GCR flux levels described in Ref. [10], we chose to test the Quad Photoreceivers with 1 GeV/n Helium up to a fluence of 1.4×10^8 cm^{-2}, and 1 GeV/n Iron ions up to a fluence of 2.8×10^5 cm^{-2}, to test the effect of GCR for a typical 10+ year long mission in outer space.

Two InGaAs Quad Photoreceivers of each diameter were manufactured for these tests, which were performed using a setup similar to the one used for the proton radiation at the NASA Space Radiation Laboratory at Brookhaven National Laboratory. The Fe and He ions were produced using an electron beam ion source and accelerated by the Booster synchrotron. Magnetic shaping yields a large flat beam spot 20 cm on a side fully containing the parts under test. The beam fluence was measured using a large planar ion chamber upstream of the targets that had been calibrated with a plastic scintillator that counted every ion passing through it. The ion beam was normally incident on three unbiased Quad Photoreceivers at ambient room temperature. The key parameters of the radiation tests are summarized in Table VII.

Table VII. GCR Constituent Ion Radiation Test Parameters

Particle	Average Flux	Irradiation Time	Fluence Level	DUT Quad Photoreceiver ID		
				0.5 mm	1 mm	2 mm
1 GeV/n Fe Ion	1.17×10^4 cm^{-2}s^{-1}	24 s	2.8×10^5 cm^{-2}	A4	B4	C4
1 GeV/n He Ion	4.78×10^5 cm^{-2}s^{-1}	293 s	1.4×10^8 cm^{-2}	A5	B5	C5

All devices subjected to 1 GeV/n Fe Ion had consistent photodiode dark current and amplifier drive current before and after radiation, as shown in Table VIII and Fig. 8. The output noise of the 0.5 mm and 1 mm diameter devices were essentially unchanged by radiation, whereas the 2 mm diameter device displayed slight increase in output noise at low frequencies around 2 MHz. All these devices were passed and reused for Gamma radiation tests described in Sec. 6.

The pre- and post-radiation tests results for the Quad Photoreceivers subjected to 1 GeV/n He Ion are shown in Table IX and Fig. 9. As is the case for the Fe Ion, the 0.5 mm and 1 mm diameter devices did not show any significant change in their performance. These two devices were passed for further radiation tests.

However, the 2 mm diameter Quad Photoreceiver (device C5) had an elevated photodiode dark current of 12.5 μA at 5 V reverse bias. The nature of the IV curve indicates breakdown of the Quad Photodiode's pn junction at ~1 V reverse bias due to displacement damage. The output noise density measurements revealed that this damage occurred in the Quadrant A of the quad photodiode chip, which not only increased the overall noise level by >50%, but also introduced substantial close-in noise at low frequencies up to 6 MHz. This corresponds to >3.5 dB degradation in signal-to-noise ratio in the entire 2 MHz to 20 MHz frequency range. It is noteworthy that the other three photoreceiver quadrants displayed normal behavior after radiation due to the probabilistic nature of device failure. Also, all four TIA circuits were undamaged by He Ion radiation. This Quad Photoreceiver was retired from further radiation tests.

Combined with the 100 MeV proton results, the GCR Ion radiation tests clearly show that larger photodiodes, which present a bigger cross-section, are more susceptible to radiation. Therefore, it is prudent to avoid unnecessarily large photodiode diameter in system design.

Table VIII. Quad Photoreceiver Results for 1 GeV/n Fe Ion Radiation with 2.8 × 10^5 cm^{-2} Fluence

Device: Quad Diameter	Condition	Total PD Dark Current @ 5V Bias (nA)	Total Amplifier Current @ ±5V Bias (mA)	Output Noise Density (nV/√Hz) per Quadrant @ 20 MHz			
				A	B	C	D
A4: 0.5 mm	Pre-Radiation	34.7	26.8	45.0	44.8	43.8	43.5
	Post-Radiation	24.7	26.6	43.5	43.0	42.0	43.8
B4: 1 mm	Pre-Radiation	64.5	26.8	62.9	65.8	63.6	61.5
	Post-Radiation	51.7	26.5	62.2	64.7	62.6	64.0
C4: 2 mm	Pre-Radiation	192.0	26.8	262.4	278.4	271.9	273.7
	Post-Radiation	179.5	26.4	262.4	268.5	276.3	277.6

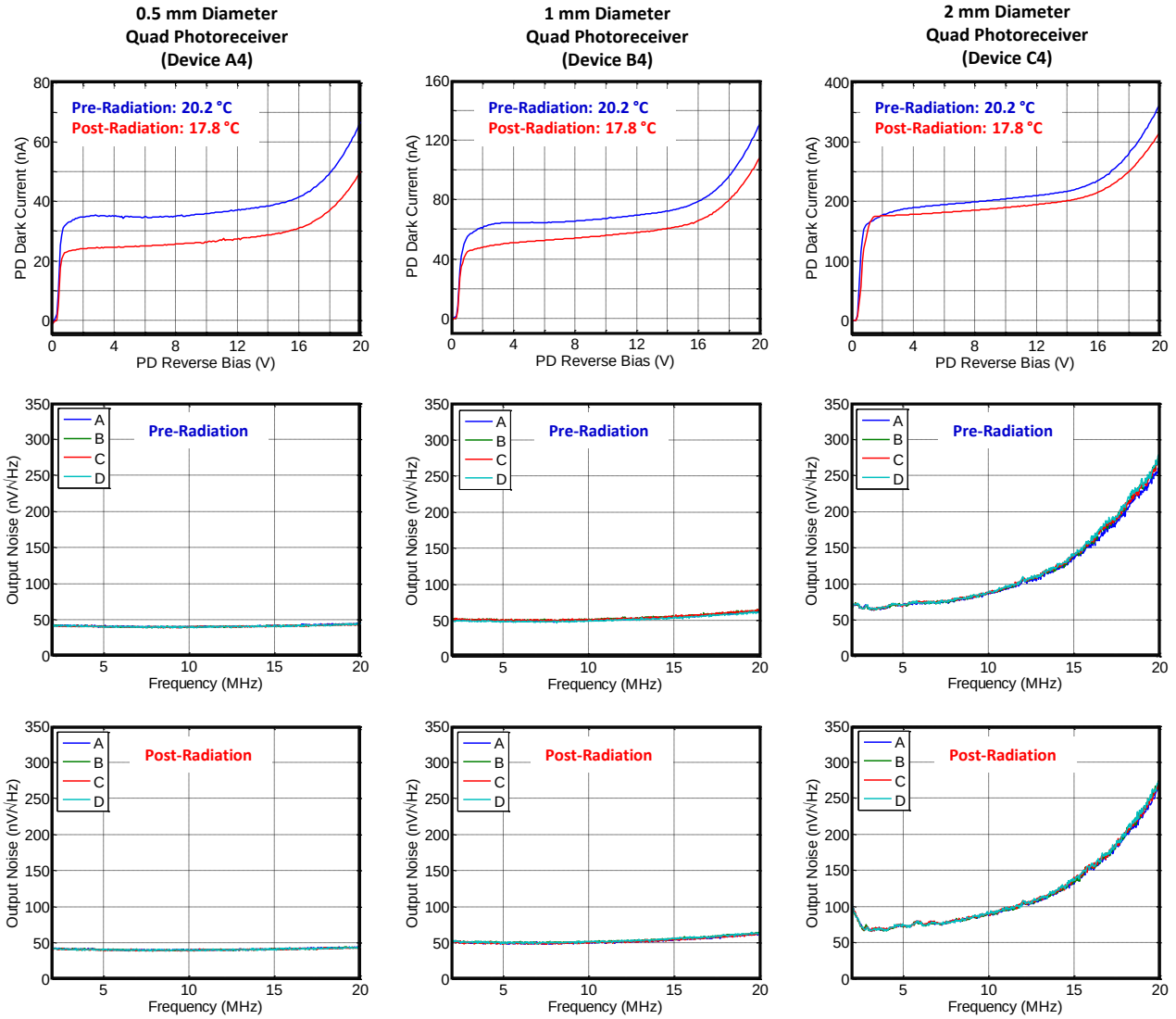

Figure 8. Combined dark current of four photodiode quadrants and output noise density spectra of Quad Photoreceivers before and after 1 GeV/n Fe radiation with 2.8 × 10^5 cm^{-2} fluence. **Note:** Minor fluctuations in dark current and output noise are observed as average room temperature is 19.5 °C ± 2 °C.

Table IX. Quad Photoreceiver Results for 1 GeV/n He Ion Radiation with 1.4 × 10^8 cm^{-2} Fluence

Device: Quad Diameter	Condition	Total PD Dark Current @ 5V Bias (nA)	Total Amplifier Current @ ±5V Bias (mA)	Output Noise Density (nV/√Hz) per Quadrant @ 20 MHz			
				A	B	C	D
A5: 0.5 mm	Pre-Radiation	36.2	26.8	44.5	44.5	43.5	43.5
	Post-Radiation	35.8	26.9	44.2	43.3	43.5	42.8
B5: 1 mm	Pre-Radiation	80.0	26.8	64.0	61.5	64.0	62.6
	Post-Radiation	87.7	27.1	62.6	60.5	61.9	62.6
C5: 2 mm	Pre-Radiation	197.8	26.8	265.0	265.0	245.5	263.0
	Post-Radiation	12547	27.0	402.5	257.5	237.8	242.0

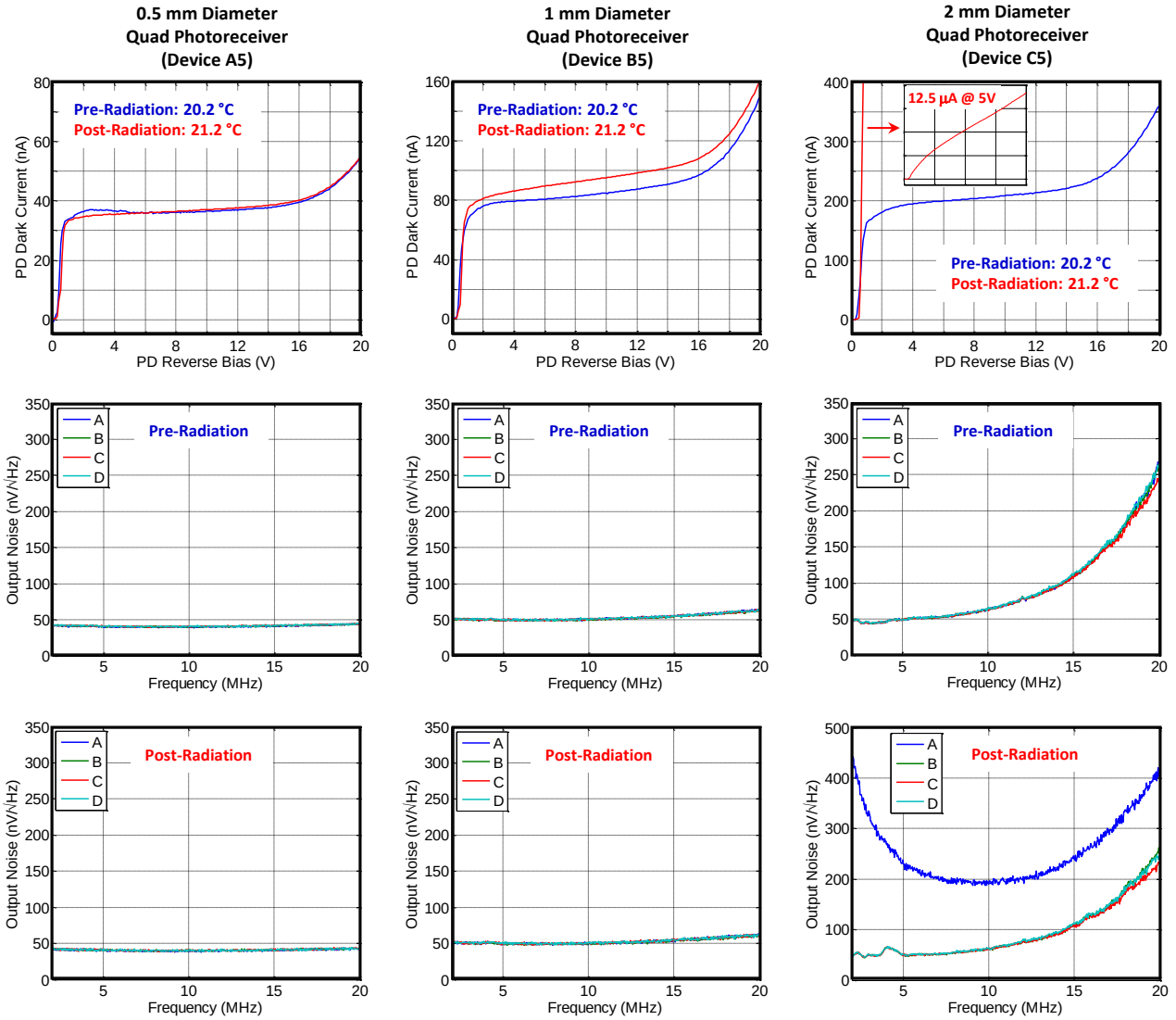

Figure 9. Combined dark current of four photodiode quadrants and output noise density spectra of Quad Photoreceivers before and after 1 GeV/n He radiation with 1.4 × 10^8 cm^{-2} fluence. **Note:** Minor fluctuations in dark current and output noise are observed as average room temperature is 19.5 °C ± 2 °C.

6. GAMMA RADIATION TESTS

The Quad Photoreceivers were irradiated with 662 keV gamma rays at the Brookhaven National Laboratory (BNL) in Upton, New York using a setup shown in Fig. 10. The same setup has been previously used to test fiber-coupled ultrafast photodetectors [4, 5]. The gamma rays are produced by a Cesium-137 source that is pneumatically raised to expose samples in a J.L. Shepherd Mark I Model 68A irradiator. The irradiator geometry accommodates sample sizes up to 12" diameter and 14" height. The dose rate is controlled by mounting the samples at one of three different positions within the irradiation chamber, and by varying the thickness of lead attenuation sheets between the source and the sample. The dose rates, expressed in rad (water) / min are regularly calibrated for each position, and are used to determine irradiation time to achieve a target total dose.

Figure 10. Photograph of J.L. Shepherd Mark I Model 68A Cesium 137 Irradiator at the Brookhaven National Laboratory used in the 662 keV gamma radiation test for the InGaAs Quad Photoreceivers (Source: www.bnl.gov/nsrl/grsf).

For our experiments, one unbiased device of each diameter was placed at the center of position #2 of the irradiation chamber for each exposure. No lead attenuation sheets were used, leading to a dose rate 141.18 rad (water) / min. The key parameters of the two gamma radiation tests are summarized in Table X. Please note that the same 2 mm diameter device, C4 was used for both exposures. Thus, the two Gamma experiments were conducted on different days so that the pre- and post-radiation performance could be measured for all conditions.

Table X. Gamma Radiation Test Parameters

Gamma Energy	Dose Rate	Irradiation Time	Total Dose	DUT Quad Photoreceiver ID		
				0.5 mm	1 mm	2 mm
662 keV	141.18 rad (water) / min	106.3 s	15.0 krad (water)	A4	B4	C4
		212.5 s	30.0 krad (water)	A5	B5	C4

As shown in Table XI and Fig. 11, the test results of all three devices were essentially unchanged by Gamma rays up to a dose of 15 krad (water). The higher dose of 30 krad (water) did not significantly impact the quad photodiodes' dark current. However, we observed 13% to 20% increase in the output noise density, corresponding to 1.1 dB to 1.6 dB degradation in signal to noise ratio, for every quadrant of the three devices (see Table XII and Fig. 12). This signifies increased input equivalent current and voltage noise of the twelve Silicon Bipolar OpAmps used in the TIA circuits of these devices. Nevertheless, these devices were deemed to pass the radiation test as the degradation in SNR was <3 dB.

Table XI. Quad Photoreceiver Results for 662 keV Gamma Radiation with TID of 15 krad (water)

Device: Quad Diameter	Condition	Total PD Dark Current @ 5V Bias (nA)	Total Amplifier Current @ ±5V Bias (mA)	Output Noise Density (nV/√Hz) per Quadrant @ 20 MHz			
				A	B	C	D
A4: 0.5 mm	Pre-Radiation	24.7	26.6	43.5	43.0	42.0	43.8
	Post-Radiation	30.9	26.6	43.2	43.0	42.5	42.3
B4: 1 mm	Pre-Radiation	51.7	26.5	62.2	64.7	62.6	64.0
	Post-Radiation	66.8	26.9	62.6	60.5	59.8	61.5
C4: 2 mm	Pre-Radiation	179.5	26.4	262.4	268.5	276.3	277.6
	Post-Radiation	199.4	26.9	251.1	266.3	263.7	268.9

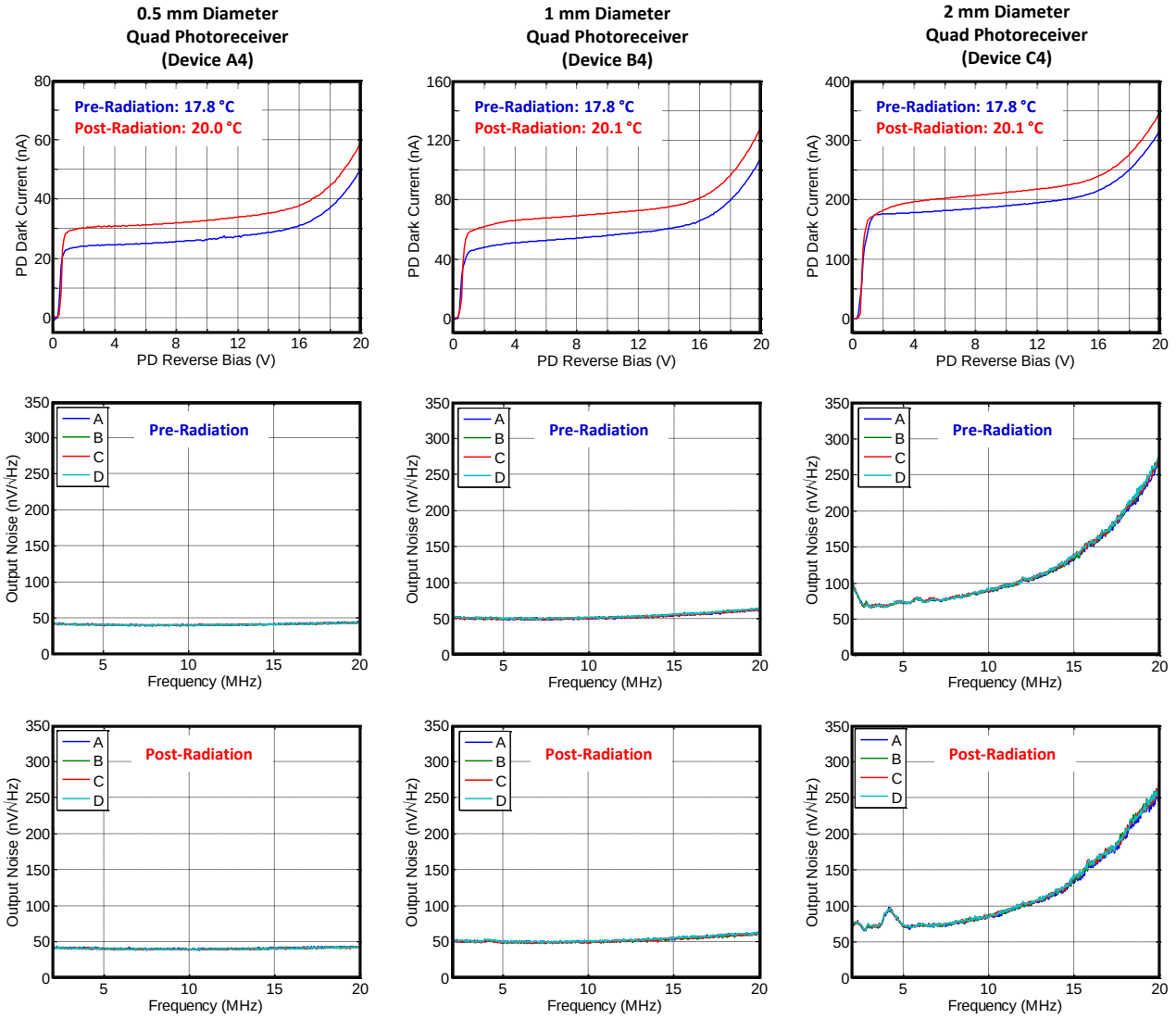

Figure 11. Combined dark current of four photodiode quadrants and output noise density spectra of Quad Photoreceivers before and after 662 keV Gamma radiation with TID of 15 krad (water). **Note:** Minor fluctuations in dark current and output noise are observed as average room temperature is 19.5 °C ± 2 °C.

Table XII. Quad Photoreceiver Results for 662 keV Gamma Radiation with TID of 30 krad (water)

Device: Quad Diameter	Condition	Total PD Dark Current @ 5V Bias (nA)	Total Amplifier Current @ ±5V Bias (mA)	Output Noise Density (nV/√Hz) per Quadrant @ 20 MHz			
				A	B	C	D
A5: 0.5 mm	Pre-Radiation	35.8	26.9	44.2	43.3	43.5	42.8
	Post-Radiation	31.5	26.7	50.3	50.0	50.8	48.3
B5: 1 mm	Pre-Radiation	87.7	27.1	62.6	60.5	61.9	62.6
	Post-Radiation	83.2	26.9	70.7	70.4	70.7	71.8
C4: 2 mm	Pre-Radiation	199.4	26.9	251.1	266.3	263.7	268.9
	Post-Radiation	210.2	26.8	300.5	310.0	316.5	315.7

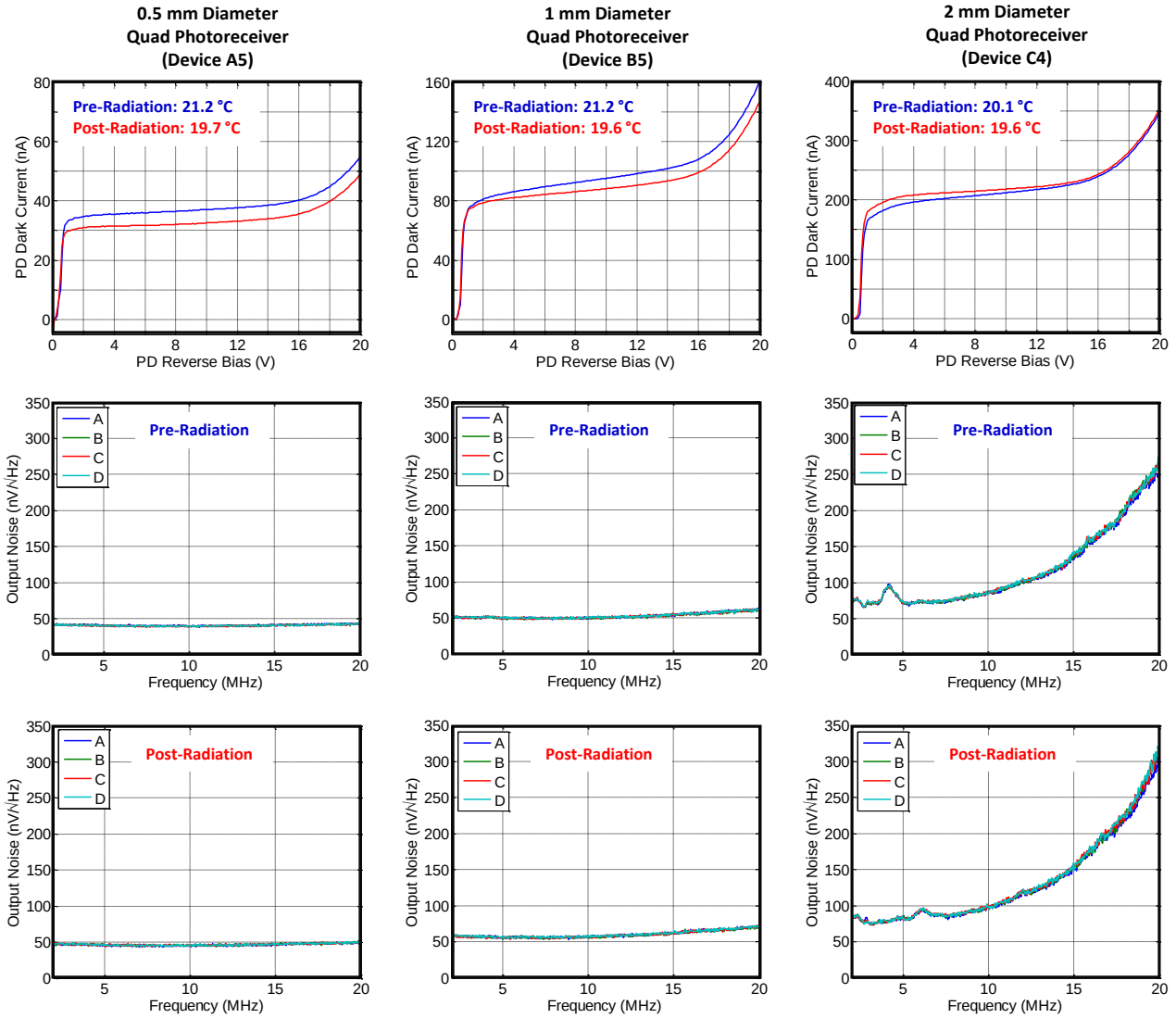

Figure 12. Combined dark current of four photodiode quadrants and output noise density spectra of Quad Photoreceivers before and after 662 keV Gamma radiation with TID of 30 krad (water). **Note:** Minor fluctuations in dark current and output noise are observed as average room temperature is 19.5 °C ± 2 °C.

7. CONCLUSION

In summary, we have developed uncooled free space coupled, ultra-low noise InGaAs Quad PD + TIA Photoreceivers that satisfy the space applications with stringent front-end sensor requirements, including gravitational wave detection. The TIA design, based on a low-noise Silicon Bipolar OpAmp, was optimized for 2 MHz to 20 MHz operation for the Laser Interferometry Space Antenna (LISA) mission. We subjected 0.5 mm, 1 mm, and 2 mm diameter Quad Photoreceivers to various radiation tests with the objective of quantifying the effect of photodiode size on resilience to radiation. The key results are listed below.

- 30 MeV Protons with fluence levels of 4.92×10^{10} cm^{-2}, 9.84×10^{10} cm^{-2}, and 1.64×10^{11} cm^{-2}: All devices passed the tests with no significant change in Quad Photodiode dark current, TIA drive current and output noise density.
- 100 MeV Protons with fluence levels of 1.27×10^{11} cm^{-2}, 2.54×10^{11} cm^{-2}, and 4.23×10^{11} cm^{-2}: All devices were functional with no significant change in output noise density and TIA drive current. However, the Quad photodiodes demonstrated >2-fold increase in dark current, thus constituting soft failure. The dark current increase due to displacement damage was especially significant for the 2 mm diameter devices.
- 1 GeV/n Fe Ion with fluence level of 2.8×10^{5} cm^{-2}: The 0.5 mm and 1 mm devices passed the test with no significant change in Quad Photodiode dark current, TIA drive current and output noise density. We observed some increase in output noise of the 2 mm diameter Quad Photoreceiver at low frequencies around 2 MHz. However, the elevated noise level at low frequencies was significantly less than the worst-case noise at 20 MHz.
- 1 GeV/n He Ion with fluence level of 1.4×10^{8} cm^{-2}: The 0.5 mm and 1 mm diameter Quad Photoreceivers passed the test with no significant change in Quad Photodiode dark current, TIA drive current and output noise density. Post-radiation, one of the quadrants of the 2 mm diameter Quad Photodiode had a very high dark current and displayed breakdown at ~1 V bias, thus constituting a hard failure. The other three quadrants of the 2 mm device displayed normal operation.
- 662 keV Gamma rays with Total Ionizing Dose (TID) of 15 krad (water) and 30 krad (water): All devices passed the test with no significant change in Quad Photodiode dark current and TIA drive current. The TIA's noise density of devices subjected to 30 krad dose increased by up to 20%, i.e. ~1.6 dB reduction in SNR, and was well within our passing criteria. The output noise density of devices subjected to 15 krad dose were essentially unchanged.

The 100 MeV proton, 1 GeV/n Fe, and 1 GeV/n He Ion radiation tests clearly show that 2 mm diameter Quad Photoreceivers are more susceptible to radiation than the 0.5 mm and 1 mm diameter devices. Therefore, it is prudent to avoid unnecessarily large photodiode diameter in system design. Combined with the earlier successful MIL-STD-883 mechanical shock and sinusoidal vibration tests, the InGaAs Quad Photoreceivers have passed preliminary testing for space qualification.

8. ACKNOWLEDGMENTS

This work was partially funded by NASA under SBIR contracts (Contract Nos. NNX09CD48P, NNX10CA59C, and NNX17CL57P). The work at NSRL is supported by NASA (Contract No. T570X) and performed under the United States Department of Energy (Contract No. DE-AC02-98CH10886). We thank Mike Lange, Lan Nguyen, and Ryan Miller for their valuable contributions in processing, assembly, and testing of these devices.

9. REFERENCES

[1] A. Joshi, S. Datta, J. Rue, J. Livas, R. Silverberg, and F. Guzman Cervantes, "Ultra-Low Noise, Large-Area InGaAs Quad Photoreceiver with Low Crosstalk for Laser Interferometry Space Antenna," Proc. SPIE, vol. 8453, paper 84532G, 2012.

[2] F. Guzman Cervantes, J. Livas, R. Silverberg, E. Buchanan, and R. Stebbins, "Characterization of photoreceivers for LISA," Classical Quantum Gravity, vol. 28, paper 094010, 2011.

[3] A. Joshi, S. Datta, N. Prasad, and M. Sivertz, "Reliability Testing of Ultra-Low Noise InGaAs Quad Photoreceivers," Proc. SPIE, vol. 10526, paper 10526-54, 2018.

[4] A. Joshi, S. Datta, R. Miller, N. Soni, M. D'Angiolillo, J. Mertz, M. Sivertz, A. Rusek, and J. Jardine, "Proton and Gamma Radiation Testing of 10 GHz Bandwidth, Uncooled, Linear InGaAs Optical Receivers," Proc. SPIE, vol. 11017, paper 11017-19, 2019.

[5] A. Joshi, S. Datta, N. Soni, M. D'Angiolillo, J. Mertz, M. Sivertz, A. Rusek, J. Jardine, S. Babu, and P. Shu, "Space Qualification of 5 to 8 GHz Bandwidth, Uncooled, Extended InGaAs 2.2 Micron Wavelength, Linear Optical Receivers," Proc. SPIE, vol. 11129, paper 11129-21, 2019.

[6] A. Joshi, J. Rue, and S. Datta, "Low-Noise Large-Area Quad Photoreceivers based on Low-Capacitance Quad InGaAs Photodiodes," IEEE Photonics Technology Letters, vol. 21, pp. 1585-1587, 2009.

[7] A. Johnston, "Radiation Effects in Optoelectronics Devices," IEEE Trans. Nuclear Science, vol. 60, no. 3, pp. 2054 - 2073, 2013.

[8] H. Becker and A. Johnston, "Dark Current Degradation of Near Infrared Avalanche Photodiodes from Proton Irradiation," IEEE Trans. Nuclear Science, vol. 51, no. 6, pp. 3572 - 3578, 2004.

[9] J. Barth, M. Xapsos, and C. Poivey, "The Radiation Environment for the LISA / Laser Interferometry Space Antenna," Document # NASA/TM-2005-212793, April 2005.

[10] R. Mewaldt, "Galactic Cosmic Ray Composition and Energy Spectra," Adv. Space Res., vol. 14, no. 10, pp. (10)737 - (10)747, 1994.